REPORT DOCUMENTATION PAGE

Public reporting burden for this collection of information is estimated to average 1 hour per response, including the time for reviewing instructions, searching existing data sources, gathering and maintaining the data needed, and completing and reviewing the collection of information. Send comments regarding this burden estimate or any other aspect of this collection of information, including suggestions for reducing this burden, to Washington Headquarters Services, Directorate for Information Operations and Reports, 1215 Jefferson Davis Highway, Suite 1204, Arlington, VA 22202-4302, and to the Office of Management and Budget, Paperwork Reduction Project (0704-0188), Washington, DC 20503.

1. AGENCY USE ONLY (Leave blank)	2. REPORT DATE APR 92	3. REPORT TYPE AND DATES COVERED QUARTERLY, 1/1/92 – 3/31/92

4. TITLE AND SUBTITLE
Quarterly Progress Report #2: 1/1/92 – 3/31/92

5. FUNDING NUMBERS
C
MDA972-91-C-0028

6. AUTHOR(S)
Dr. Ching-Tzong Sune
Gary W. Jones, Principal Investigator

7. PERFORMING ORGANIZATION NAME(S) AND ADDRESS(ES)
MCNC Electronic Technologies Division
Post Office Box 12889
3021 Cornwallis Road
Research Triangle Park, North Carolina 27709-2889

8. PERFORMING ORGANIZATION REPORT NUMBER
P9250004-Q2

9. SPONSORING ORGANIZATION NAME(S) AND ADDRESS(ES)
ARPA/DSO
3701 North Fairfax Drive
Arlington, Virginia 22203-1714

10 SPONSORING/MONITORING AGENCY REPORT NUMBER

11. SUPPLEMENTARY NOTES
Dr. Sune (919) 248-1975, (919) 248-1455 FAX
COTR: Dr. Bertram Hui (703) 696-2239, (703) 696-2201 FAX

12a. DISTRIBUTION/AVAILABILITY STATEMENT
Approved for public release; distribution is unlimited.
Defense Technical Information Center
Building 5 / Cameron Station
Arlington, Virginia 22214

12b. DISTRIBUTION CODE
A

13. ABSTRACT (Maximum 200 words)

Second Quarterly R&D Status / Technical report for the Field Emitter Array RF Amplifier Development Project - Phase I, Cathode Technology Development.

DTIC SELECTED DEC 07 1995 B

19951205 087

14. SUBJECT TERMS
Field emission, cold cathode, RF amplifier

15. NUMBER OF PAGES
19

16. PRICE CODE

17. SECURITY CLASSIFICATION OF REPORT	17. SECURITY CLASSIFICATION OF THIS PAGE	17. SECURITY CLASSIFICATION OF ABSTRACT	20. LIMITATION OF ABSTRACT
UNCLASSIFIED	UNCLASSIFIED	UNCLASSIFIED	

NSN 7540-01-280-5500

MCNC Field Emitter Array RF Amplifier Development Program
Phase One, Cathode Technology Development - DARPA Contract MDA 972-91-C-0028

Second Quarter - March 1992

MCNC Silicon Field Emitter with Column

Insulator 1

Emitter Tips

Insulator 2

Extractor

Silicon

Key Ideas

Develop microstructural field emission diodes with a cutoff frequency above 1 GHz, 5A/cm^2 at <200V G-E bias, and >100hr lifetime.

Reduce capacitance and increase transconductance of FEA devices to improve frequency response. Primarily use tall emitter columns surrounded by SiO$_2$ to reduce capacitance. Evaluate low work function emitter surfaces, small gate dimensions, and improved tip radius control to improve transconductance.

Evaluate various anode configurations including vacuum microencapsulation to permit testing of larger numbers of sample FEA devices.

Model and characterize our versions of the FEA device.

Major Accomplishments:

Gated field emitter-on-a-column structures with low capacitance have been successfully fabricated. Testing is about to begin.
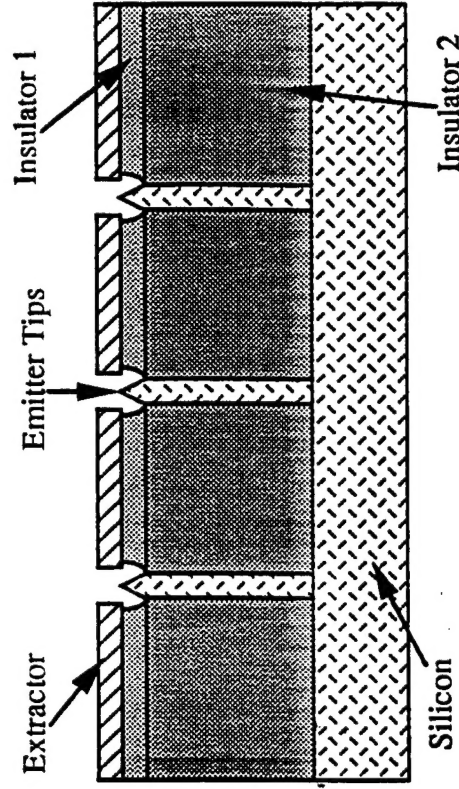
Two isotropic silicon emitter etches have been successfully explored. One has been implemented into the gated silicon column structure.

Early versions of field emission triodes which have been vacuum micro-encapsulated have been built successfully.

A microstrip packaging design methodology has been designed to null capacitance in FEAs for narrow band, high frequency applications. 10-20 GHz may be possible using 1 μS low capacitance FEAs with a >700MHz bandwidth.

Testing of silicon tips with various surface treatments has produced one possible low voltage (~10V) /high transconductance (>100 μS) FE diode design. More testing is required to verify these very recent results.

Major Milestones - This quarter and upcoming quarter

Construction of low capacitance gated FEA structure with 1.2 micron gates (3/92-complete). Testing planned for next quarter (first pass testing planned for completion by 6/92)

Complete first pass RF models for FEA devices (3/92 - complete)

Complete new FEA mask set (planned 5/92 - complete)

Obtain g$_m$/C suitable for 1 GHz (planned 9/92 - ahead of schedule, in verification stage, now planned for 6/92)

Insertion of FEAs in macroscale tubes (planned 3/92 - now planned for 6/92) - Task expanded to both triodes and microstrip cavities.

Delivery of vacuum microencapsulation system (planned 4/92 - on schedule), Complete setup of vacuum microencapsulation system (planned 8/92 - on schedule)

Field Emitter Array RF Amplifier Development Project
Phase 1, Cathode Technology Development

I. Executive Summary

- Gated field emitter-on-a-column structures with low capacitance ($< 10^{-15}$ F/cell) have been successfully fabricated. Columns of 6 microns final height were built based on data indicating the taller columns were of marginal added benefit. Testing is about to begin.

- Two isotropic silicon emitter etches have been successfully explored. One has been implemented into the gated silicon column structure.

- Early versions of field emission triodes which were vacuum micro-encapsulated have been successfully built. Turn-on was as low as 20 volts. A paper was written on these thin film encapsulated FEA devices and submitted to the Electronic Components and Technology Conference. A copy of the paper was sent to the DARPA contract administrator. This paper will be given in San Diego in May of 1992. Vacuum microencapsulated devices fabricated using the new vacuum sealing tool, which is due in April, should perform at near open diode performance levels. They will have a greater than 100 micron gate-to-anode spacing.

- A 0.6 micron gate opening mask has been fabricated which will provide ~2,000,000 tips in a 4x4 mm array, and will provide ~0.3-0.5 micron gate-to-emitter tip spacing on top of the low capacitance columns.

- A microstrip packaging design methodology has been designed to null capacitance in FEAs for narrow band, high frequency applications. A frequency of 10-20 GHz may be possible using 1 μS low capacitance FEAs with a >700 MHz bandwidth. This work was performed by Bill Joines at Duke University. This concept is apparently common in the III-V industry and will be applied to devices packaged at Litton Solid State.

- Testing of silicon tips with various surface treatments produced apparent low voltage (~10V) / high transconductance (>100 μS) FE diode arrays (Figure 1). Further evaluation of these results indicated that there was an error in our testing set-up and evaluation criteria. Once the test set-up was corrected and the anode was truly separated, very small anode current was detected. The devices exhibited a diode leakage across the oxide which was higher than the typical Frankle-Pool leakage. Samples of these diodes have been sent to Henry Gray for testing. Work on emitter surface treatments will continue.

- Emitter treatments to lower work function to-date have provided negligible improvement or degraded the emitter characteristics. Further evaluations of emitter treatments with remote plasmas and thin film emitter coatings are planned.

Availability Codes	
Dist	Avail and/or Special
A-1	

II. Milestone Status:

Task	Completion Date	
	Original	Complete Expected
Complete first diodes of each of the three device types: Horizontal, vertical, and trench. Deliver samples to NRL, NCSU, and Litton. (MCNC)	11/91	11/91
Prepare first pass device models and potential circuit models based on initial device IV data. (Duke, MCNC, and UNC-CH)	3/92	11/92
Down select RF FEA designs based on device performance predictions	3/92	12/91
Complete first generation of field emission I-V curves for each of the device types fabricated along with initial electron trajectory data and electron time of flight data. (NCSU and MCNC)	3/92	3/92 (time of flight planned 6/92)
Design and order vacuum sealing and test system (MCNC)	11/92	12/91
Modify Litton trajectory modeling programs for field emission. Initial macroscale high vacuum tube encapsulation of field emission cathodes. (Litton)	3/92	11/91
Complete second set of field emission diode device runs with column FEAs (MCNC)	3/92	3/92
Complete new mask set for half micron field emission devices. (MCNC)	5/92	3/92
Install vacuum sealing and test system (MCNC)	3/92	4-5/92
Complete initial electron trajectory modeling and initial testing of macroscale tubes containing microstructural gated FEC diodes. (Litton)	7/92	7/92
Complete fabrication of first microencapsulated FEC transistors. (MCNC)	9/92	9/92
Generate first pass transistor data from microencapsulated FE transistors. (MCNC, Duke, and Litton)	9/92	9/92
Construct microstructural FEA devices meeting device IV and g_m/C requirements.	9/92	9/92
Determine priorities of future device development. Determine the primary amplifier design methodology from the three amplifier design approaches. (MCNC)	9/92	9/92
Complete design for first integrated FEC based RF amplifier and FEC tube RF amplifier based on device characterizations. (MCNC, Duke, and Litton)	3/93	3/93
Complete second level models for FEC emission from surfaces treated in various manners. (UNC-CH)	3/93	3/93
Complete testing of FEC electron trajectories, electron trajectory model verification. (NCSU, Litton)	3/93	3/93
Determine packaging and cooling requirements for the prototype RF amplifier. (MCNC and Litton)	3/93	3/93

III. Technical Progress:

1.0 Theoretical FEA device developments

1.1 A model of an array of emitter tips on columns of 3, 5.7, and 9.7 microns in height and with variable spacing was performed by Bill Joines at Duke University to evaluate the potential of arrays of grouped emitters with a separate extraction grid. Maximum current densities occurred at emitter height and

spacings of 2-3 times the height of the emitter column. This optimum spacing was shown to be ~15 microns for a ~6 micron tall column.

1.2 A method for packaging FEA devices was modeled by Bill Joines at Duke University which permits the nulling of the emitter-gate capacitance. This method uses strip line inductance to null parasitic capacitance and to obtain higher cuttoff frequencies at the expense of bandwidth. This technique has been used extensively in other microstrip-based microwave amplifier applications. The high power gain of the FEA permits reasonable gain bandwidth products even with low transconductance/capacitance per cell ratios. These models predict a ~700 MHz bandwidth in the range of 10 - 20 GHz, although one must preselect the target frequency to be amplified. An attachment showing several examples of this technique applied to FEAs is included as Attachment A.

2.0 Field Emitter Development

2.1 A new emitter mask has been built which will permit 0.4-0.6 micron diameter emitter columns to be built with 0.6-1.0 micron diameter gate openings. This mask matches the other recently constructed masks and will permit higher density, higher transconductance emitter arrays to be built. Within the 1 cm^2 chip area, there are a variety of different size FE arrays ranging from 1 emitter per cell to over 2,000,000 emitters in a 4 mm X 4 mm cell.

2.2 Fabrication of columnar gated emitters
Gated columnar emitters have been fabricated which are imbedded in a silicon dioxide matrix. These devices have 6 micron high columns which were previously modeled to be within 20-30% of the theoretical minimum-per-cell capacitance for a given gate-to-emitter spacing. The gate to emitter spacing is smaller on these devices than our non-column arrays. Our previous emitters had a 2.2 micron gate opening, while these possess a 1.2 micron gate opening. A series of in-process SEMs is shown in Figure 2. This process appears robust and accurately permits both horizontal and vertical self-aligned placement of small diameter, tall emitters.

3.0 Vacuum Sealing/Testing System Design

3.1 Field emitter arrays of up to 16 emitters have been micro-encapsulated using thin film techniques. These devices exhibited triode characteristics. The performance of these devices was poor due to low transconductance (0.1 µS) and anode field penetration which turned on the emitter at voltages near the gate turn-on. Leakage was near or below our measurement sensitivity between the emitters and the gate as well as emitters and the anode. Anode to gate separation was only 3 microns in these test devices. These performance effects were attributed to emitter contamination left from the resist spacer removal process and the close proximity of the emitter to the anode. Micro-encapsulated emitter array triodes produced by the new vacuum bonder are expected to provide electrical characteristics similar to or better than those of open diodes.

4.0 Other Developments

4.1 The Litton triangular mesh computer simulation program (DEMEOS) has been modified with recent data and improved emission models to provide agreement with observed MCNC experimental gated diode characteristics. Continued improvements during the next quarter will aid in the incorporation of these diodes into amplifier tubes.

4.2 The Litton Solid State Division met with the Electron Devices Group and MCNC to determine how to best package FEA chips. Two techniques are to be attempted which are similar to those previously proposed. First, Litton SSD will lay out a microstrip mounting which will be placed in one of their standard coaxially connected RF cavities. MCNC will prepare titanium coated foil anodes and also send Litton some additional emitter arrays, Litton EED will vacuum seal this cavity.

The second technique was a refinement of the vacuum tube approach. A series of small vacuum tubes will be fabricated using glass sealing with remote anodes in high vacuum at Litton EED. This will permit testing of a larger number of samples prior to construction of more complex tubes.

Both these encapsulation approaches are expected to be completed and tested prior to the end of the next quarter.

4.3 UNC-Charlotte has been building their vacuum test system during the past quarter. The Electrical Engineering Department at UNC-Charlotte is funding purchase of these parts. This system will be used to evaluate noise on emitter tips produced at MCNC.

A theoretical analysis of emitter noise by Richard Greene accompanies this report as Attachment B. It provides a possible explanation for emitter noise observed by other researchers. Noise from MCNC devices has not yet been studied, but experimental work using the new system is planned.

4.4 North Carolina State University has brought their electron trajectory system on line and has started characterizing free-standing and gated emitters. Tests using free-standing silicon emitters have shown nearly identical electrical characteristics over a wide range of temperatures from 250 C to 33 C (see Figure 3). Initial data taken on single emitters closely matches results obtained by Henry Gray on single silicon emitters.

An unusual diode leakage characteristic was observed (Figure 6) during testing at NCSU on one group of samples. The nature of this leakage has not been determined, but will be studied further.

IV. Fiscal Status
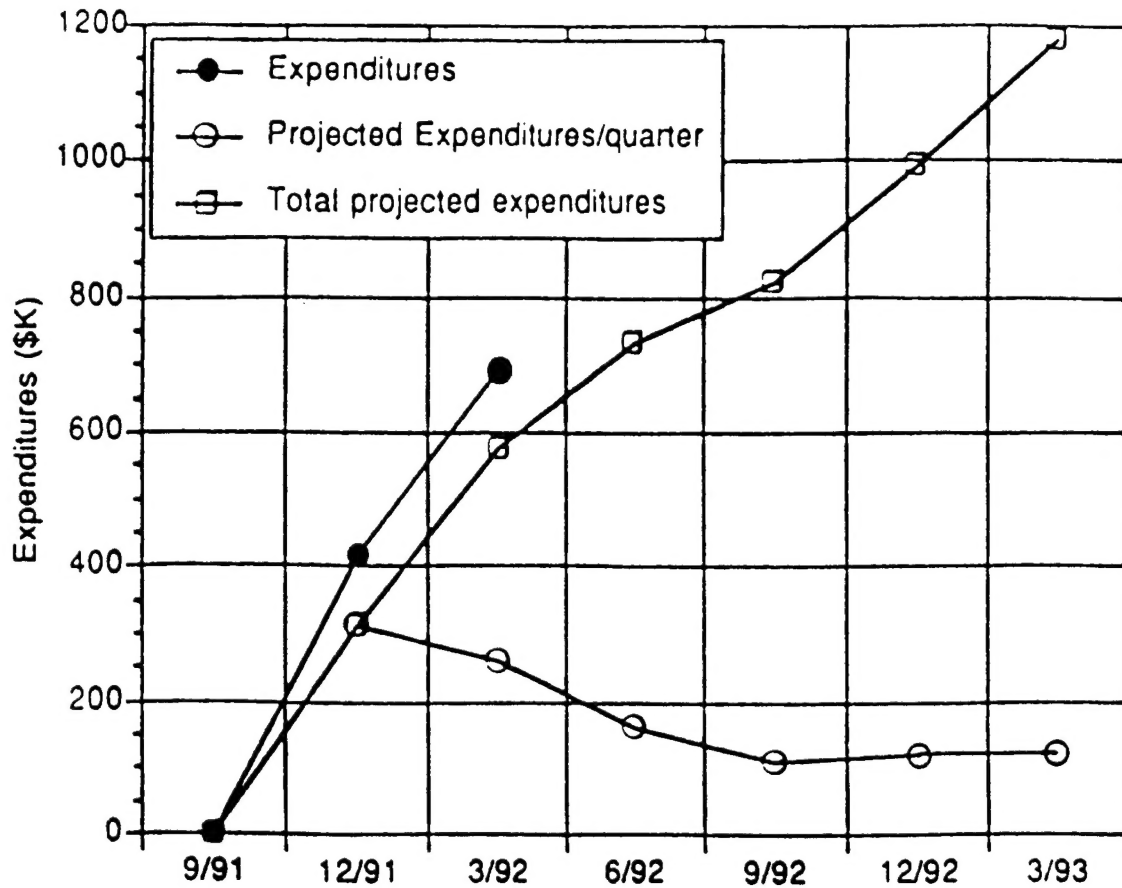
Expenditures this quarter (1/1/92 - 3/31/92)	$280,773.52
Total expenditures to date (9/9/91 - 3/31/92)	693,852.03 *
Projected expenditures:	
4/92 - 6/92	141,676.12
7/92 - 9/92	107,469.85
10/92 - 12/92	117,734.00
1/93 - 3/93	117,734.00
Contract Amount (Basic)	$1,178,466.00

* Amount does not include processing costs for March 1992.

V. Problem Areas

The initial 1 GHz objective theoretically appears achievable with our current device design and emitter material selection. Long term >10GHz Phase 2 objectives may require the use of optimal device packaging techniques which permit the nulling of emitter-to-gate capacitance at the expense of bandwidth. Lowering the emitter surface work function continues to a major goal along with reducing the emitter-to-gate spacing. Several techniques for lowering the work function are still being explored. Devices with smaller gate openings are under construction. Alternative beam focusing and deflection based devices which do not require modulation of emission are still under review for >>20 GHz applications.

VI. Visits and Technical Presentations

The only presentation made on this project outside the direct program participants during the contract time period has been the DARPA second meeting review. Numerous closed meetings were held between MCNC staff and its subcontractors. No visitors have reviewed this project.
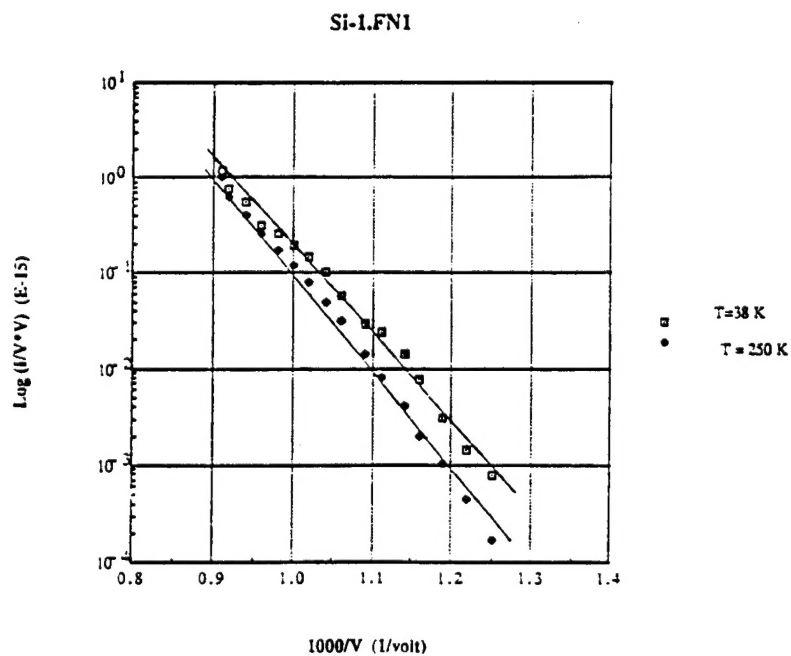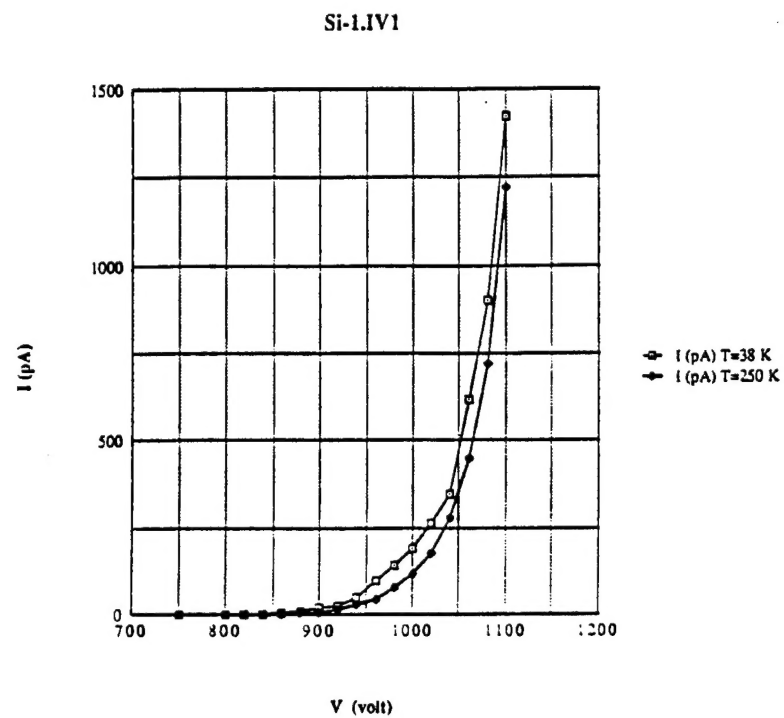
Si-1.IV1

Si-1.FN1

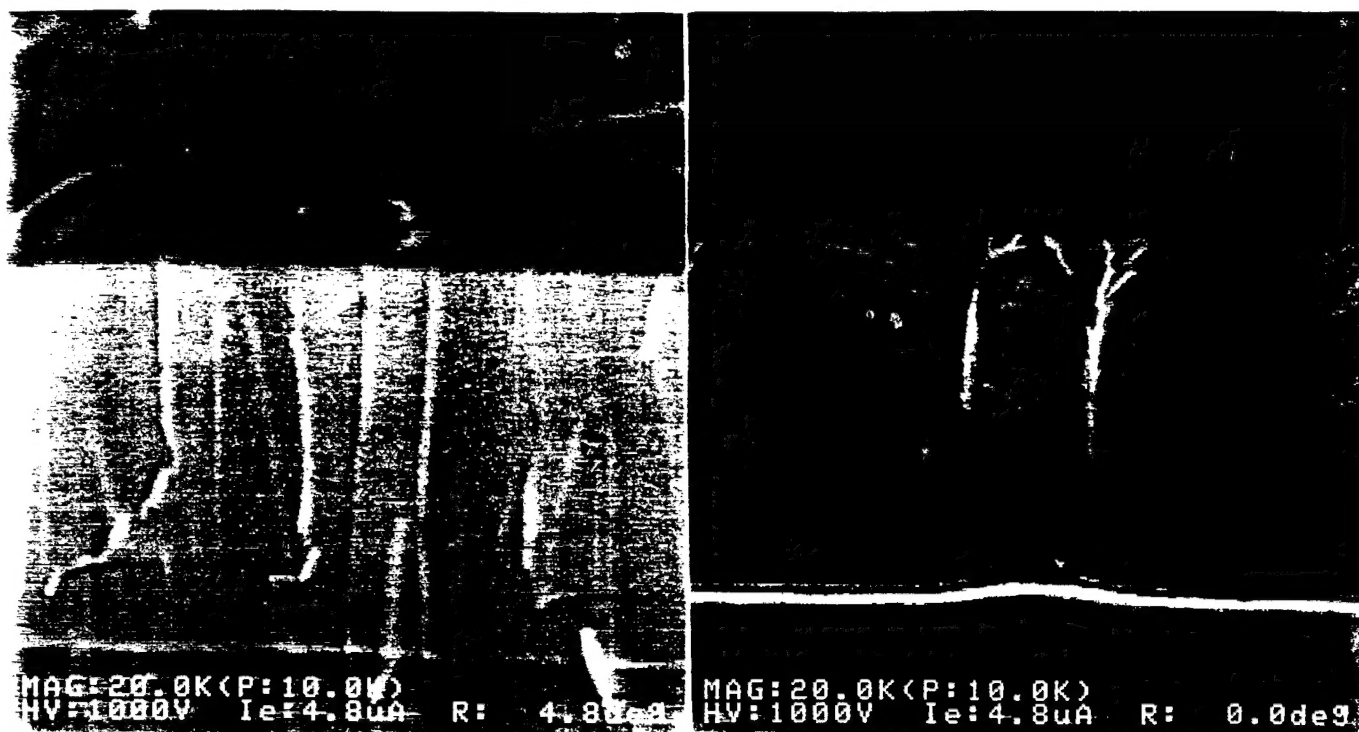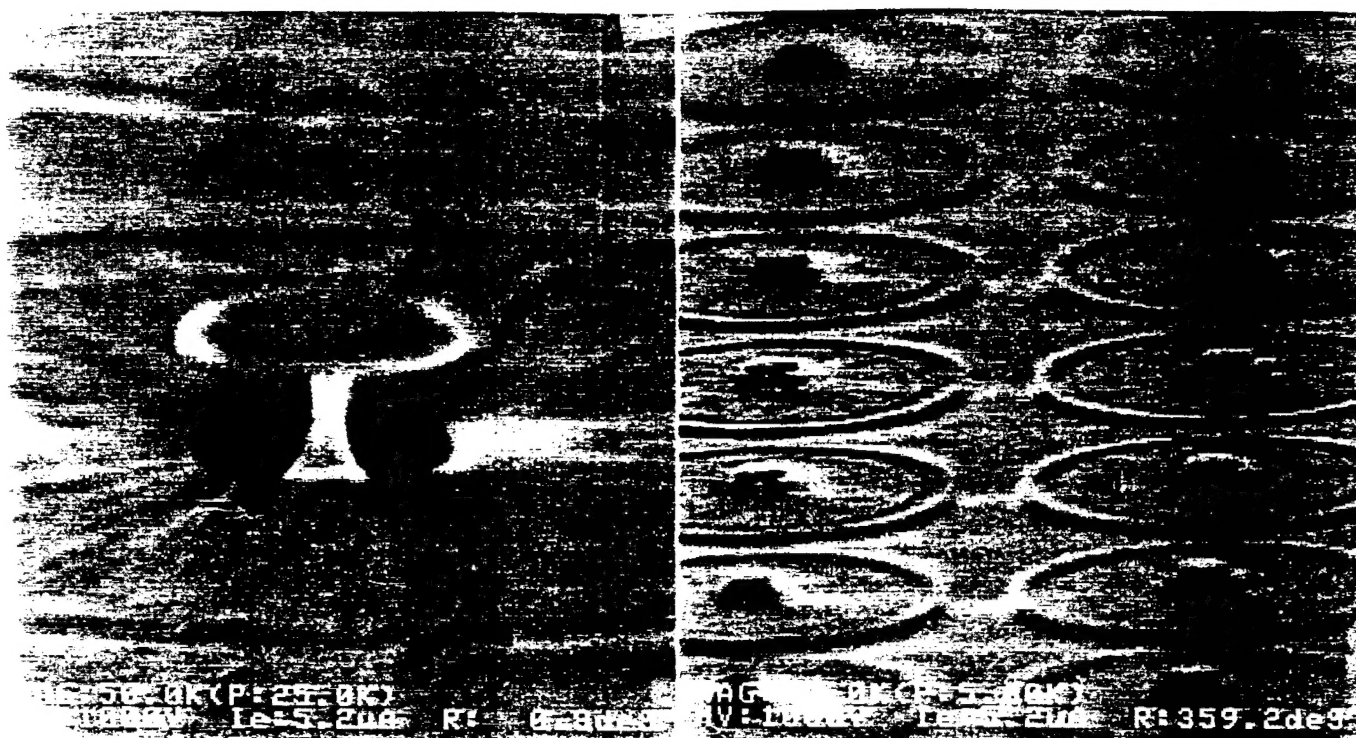Fig. 2 I-V characteristics and F-N plot of a single Si tip.

Figure 3

Top Left: Emitter column with cap still in place prior to second layer dielectric and metal deposition
Top Right: Array of emitter caps on silicon columns in oxide matrix
Bottom Left: Emitter cap on column in oxide matrix
Bottom Left: Cross section of emitter tip on silicon column in silicon dioxide matrix

Attachment A

RESONANT OR TUNED FIELD EMITTER AMPLIFIER

William T. Joines and Joseph E. Mancusi
Duke University, 2/29/92

1   EQUIVALENT CIRCUIT AND GAIN AT RESONANCE

An equivalent circuit of the field-emitter amplifier (FEA) is shown in Fig. 1a, where the interelectrode capacitances and resistances (R_1 and C_1 on the input side, and R_2 and C_2 on the output side) are indicated. The inductances L_1 and L_2 are added external to the device for the purpose of resonating with, and therefore nulling out the effects of, C_1 and C_2 at any selected frequency f_0. The conditions at resonance (f_0), the gain versus frequency, the frequency bandwidth, and the physical realization of the tuned amplifier will be examined.

1.1   Gain at resonance

With reference to Fig. 1a, at resonance ($f = f_0 = \frac{\omega_0}{2\pi}$):

$$\omega_0 L_1 = \frac{1}{\omega_0 C_1} \tag{1}$$

and

$$\omega_0 L_2 = \frac{1}{\omega_0 C_2} \tag{2}$$

This leaves the input and output impedances at f_0 as just R_1 and R_2, respectively, as indicated in Fig. 1b. From this simple circuit one obtains:

$$\frac{v_{ge}}{v_S} = \frac{R_1}{R_1 + R_S} \tag{3}$$

$$\frac{v_L}{v_{ge}} = -g_m \frac{R_2 R_L}{R_2 + R_L} \tag{4}$$

and

$$\frac{v_L}{v_S} = -g_m \frac{1}{1 + \frac{R_S}{R_1}} \frac{1}{\frac{1}{R_2} + \frac{1}{R_L}} \tag{5}$$

or

$$\frac{v_L}{v_S} \cong -g_m R_L \tag{6}$$

1

since $R_S \ll R_1$ and $R_L \ll R_2$. Thus, by nulling out the effects of C_1 and C_2 with L_1 and L_2 at $f = f_0$, the highest gain that the amplifier is capable of producing ($g_m R_L$) may be realized at any selected frequency f_0.

In example calculations that follow here and in later sections, it is assumed that $g_m = 25$ mS (the transconductance of about 30,000 emitters), $C_1 = 4$ pF, $C_2 = 2$ pF (the total capacitances contributed by about 30,000 emitters), $R_S = 50\Omega$, and $R_L = 50\Omega$. If needed, R_S and R_L may be made to appear smaller or larger by using quarter-wavelength transformers at $f = f_0$. Hence, using the parameter values given, the gain at f_0 is:

$$\frac{v_L}{v_S} \cong -g_m R_L = -0.025 \times 50 = -1.25 \tag{7}$$

If a quarter-wavelength ($\lambda_0/4$) transformer of say 150Ω characteristic impedance is placed between the amplifier output and the 50Ω load, the effective load resistance becomes $(150)^2/50 = 450\Omega$, which raises the amplifier gain at f_0 to:

$$\frac{v_L}{v_S} \cong -0.025 \times 450 = -11.25 \tag{8}$$

2 GAIN VERSUS FREQUENCY AND BANDWIDTH

The gain versus frequency is obtained by including all of the elements in Fig. 1a to obtain:

$$\frac{v_{ge}}{v_S} = \frac{Z_1}{Z_1 + R_S} = \frac{1}{1 + R_S Y_1} \tag{9}$$

$$\frac{v_L}{v_{ge}} = -g_m \frac{Z_2 R_L}{Z_2 + R_L} = \frac{-g_m R_L}{1 + R_L Y_2} \tag{10}$$

and

$$\frac{v_L}{v_S} = \frac{1}{1 + \frac{R_S}{Y_1}} \frac{-g_m R_L}{1 + R_L Y_2} \tag{11}$$

The denominator terms may be expressed as:

$$1 + R_S Y_1 = 1 + R_S \left(\frac{1}{R_1} + j\omega C_1 + \frac{1}{j\omega L_1} \right) = \frac{R_1 + R_S}{R_1} \left[1 + j Q_1 \left(\frac{f}{f_0} - \frac{f_0}{f} \right) \right] \tag{12}$$

and

$$1 + R_L Y_2 = 1 + R_L \left(\frac{1}{R_2} + j\omega C_2 + \frac{1}{j\omega L_2} \right) = \frac{R_2 + R_L}{R_2} \left[1 + j Q_2 \left(\frac{f}{f_0} - \frac{f_0}{f} \right) \right] \tag{13}$$

where

$$Q_1 = \omega_0 C_1 R_1 R_S / (R_1 + R_S) \tag{14}$$

and

$$Q_2 = \omega_0 C_2 R_2 R_L / (R_2 + R_L) \tag{15}$$

Substituting back into the gain equation yields:

$$\frac{v_L}{v_S} = \frac{-g_m R_L (R_1 R_2)/[(R_1 + R_S)(R_2 + R_L)]}{\left[1 + jQ_1\left(\frac{f}{f_0} - \frac{f_0}{f}\right)\right]\left[1 + jQ_2\left(\frac{f}{f_0} - \frac{f_0}{f}\right)\right]} \tag{16}$$

Again, since $R_S \ll R_1$ and $R_L \ll R_2$, the gain becomes $-g_m R_L$ at $f = f_0$. Also, Q_1 and Q_2 are approximately,

$$Q_1 \cong \omega_0 C_1 R_S \tag{17}$$

and

$$Q_2 \cong \omega_0 C_2 R_L \tag{18}$$

Since $C_1 > C_2$, Q_1 limits the bandwidth more than Q_2, and the 3-dB bandwidth is determined from:

$$Q_1 \cong \omega_0 C_1 R_S = f_0/BW \tag{19}$$

With $C_1 = 4$ pF and $R_S = 50\Omega$, the 3-dB bandwidth at any f_0 is:

$$BW = 1/(2\pi C_1 R_S) = 0.795 \; GHz = 795 \; MHz \tag{20}$$

If R_L is transformed up from 50Ω to 450Ω and $C_2 = 2$ pF, then $Q_2 > Q_1$ and th 3-dB bandwidth at any f_0 becomes:

$$BW = f_0/Q_2 = 1/(2\pi C_2 R_L) = 0.177 \; GHz = 177 \; MHz \tag{21}$$

3 PHYSICAL REALIZATION OF TUNED AMPLIFIER

The inductances L_1 and L_2, that are used to null out the effects of C_1 and C_2 at any selected frequency, are easily incorporated into the microstrip circuit that will be used in testing the field-emitter amplifiers. Fig. 2 shows the microstrip circuit with a packaged amplifier (grid, emitter, and collector leads) to be inserted. The input and output RF lines are of 50Ω characteristic impedance ($w_0 = 2.44$ mm on the 0.723 mm thick, RT Duroid dielectric substrate). The open-circuited stubs of physical length l_1 and l_2 are between one-quarter and one-half wavelength long at f_0 and form the inductances L_1 and L_2. For example calculations these stubs will also be assigned a characteristic impedance of 50Ω, which can be changed to make the physical lengths longer or shorter if desirable. The physical lengths l_1 and l_2 are:

$$l_1 = \frac{\lambda}{2\pi}\tan^{-1}\left(\frac{-Z_{01}}{\omega_0 L_1}\right) = \frac{\lambda}{2\pi}\tan^{-1}\left(-Z_{01}\omega_0 C_1\right) \tag{22}$$

and

$$l_2 = \frac{\lambda}{2\pi}\tan^{-1}\left(\frac{-Z_{01}}{\omega_0 L_2}\right) = \frac{\lambda}{2\pi}\tan^{-1}\left(-Z_{01}\omega_0 C_2\right) \tag{23}$$

3

If $Z_{01} = 50\Omega$, $C_1 = 4\ pF$, and $C_2 = 2\ pF$, then:

$$l_1 = \frac{\lambda}{2\pi} \tan^{-1}\left(-1.257 f_{0G}\right) \qquad (24)$$

and

$$l_2 = \frac{\lambda}{2\pi} \tan^{-1}\left(-0.6285 f_{0G}\right) \qquad (25)$$

where f_{0G} is the selected frequency in GHz. At 10 GHz, $\lambda = 21.93$ mm for the 50-ohm microstrip lines in Fig. 2, thus, the physical lengths at 10 GHz are:

$$l_1 = 0.263\lambda = 5.77\ mm \qquad (26)$$
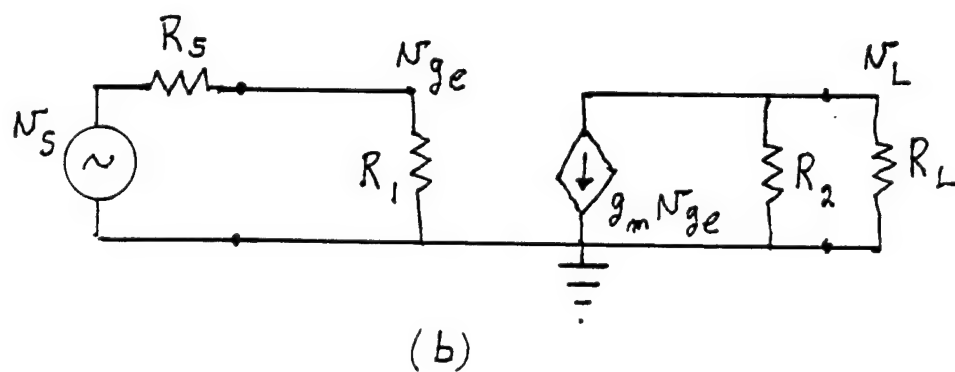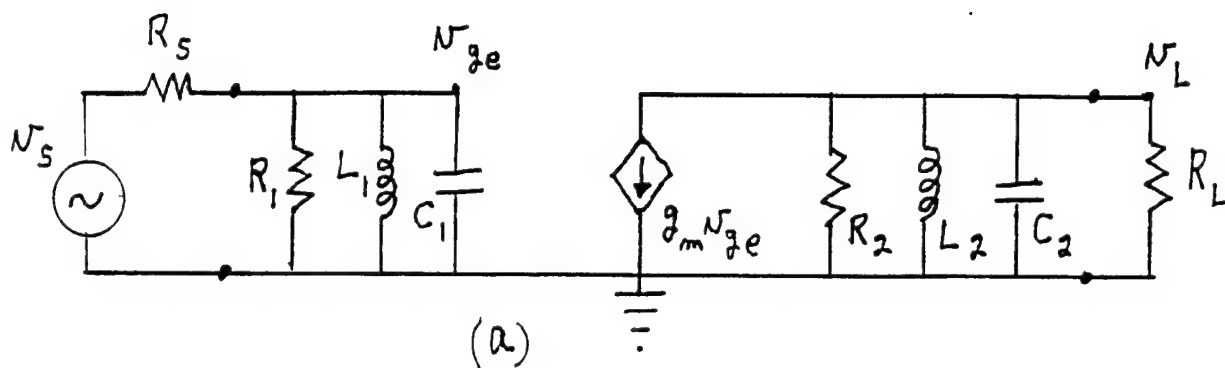
and

$$l_2 = 0.275\lambda = 6.03\ mm \qquad (27)$$

Figure 1: Amplifier equivalent circuit (a) with all elements included, and (b) at $f = f_0$, where $\omega_0 L = 1/(\omega_0 C)$ for both the input and output circuits.
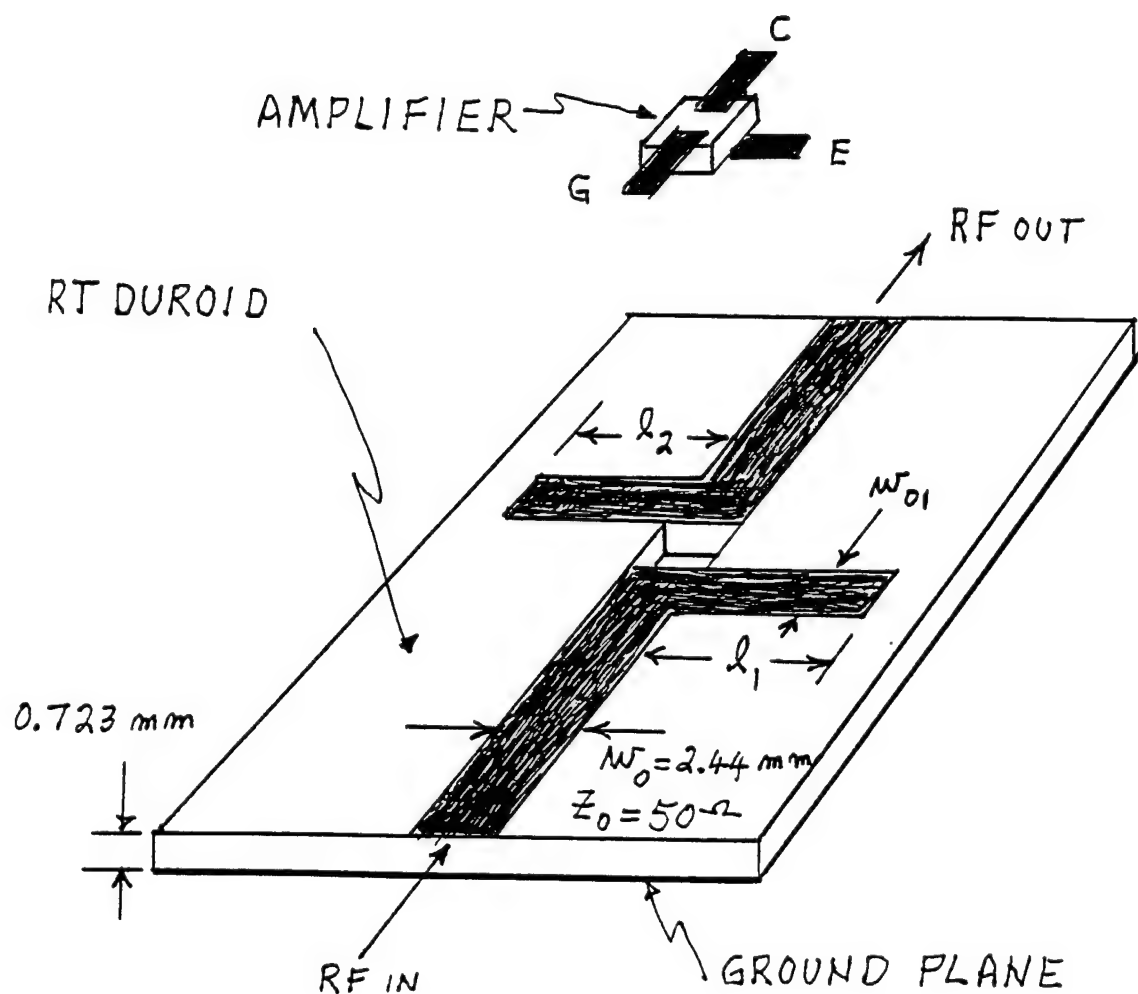
Figure 2: Microstrip circuit for testing the amplifier that is to be inserted into the space provided. The open-circuited stubs of length l_1 and l_2 provide the resonating inductances L_1 and L_2.

Attachment B

DARPA PROGRESS REPORT 3/14/92

1/f NOISE IN FIELD EMISSION
R. F. Greene,
ELECTRICAL ENGINEERING DEPARTMENT
University of North Carolina at Charlotte

CONTENTS:

1.   INTRODUCTION: One of the technical questions which must be answered in the quest for
a technically significant vacuum microelectronics is the issue of noise in field emission, what
its origin is, how it might be controlled, and how it will affect the operation of microwave
amplifiers using arrays of emitters.   The issue of the origin of flicker noise from metals is
addressed in this report, and a model calculation is proposed which makes preictions which can
be checked against experiment.   If the theory is substantiated by experiment, the effect on
device characteristics can be calculated, and strategies for noise reduction undertaken.   The
outline of a theory is given here and it is pointed out that our model does provide a prediction of
noise spectral density and amplitude and the dependence of these noise characteristics on
experimental conditions.   Numerical evaluation of the formulas will be subsequently carried
out and reported.
        Several investigators [1,2,] have observed "flicker noise", i.e. current fluctuations
with a 1/f power spectrum in field emission from both semiconductor and metal emitter tips.
(High frequency emission noise has been analyzed previously [3]) The intensity generally
decreases strongly with pressure as one gets well into the UHV regime. Furthermore, Gray [4]
has reported the observation of "search-light effects" in field emission at intermediate vacuum
levels: this is the sudden change in emission direction seen on the phosphor screen of an
emission microscope. Observations many years ago by R. Gomer[5], showed that emission
fluctuations could be correlated with surface diffusion of adatoms, as seen in field electron
microscopy.   It is the purpose of this work to unite these observations within the framework of
a theory of field emission as affected by adatoms. (We use only the simplest tunneling
theory.)In addition, we have to bring into the same framework the observation of emission
current fluctuations associated with the "forming process" observed by Egorov [6].

2.   CALCULATION OF ADATOM CONTRIBUTION TO FIELD EMISSION: We will simply
superpose upon the ordinary Folwer-Nordheim tunnelling current an extra current due to the

presence of an adatom. The model takes into account two effects: a). As is well-known, many adatoms are polarized by the effect of the work function on the atomic orbitals of the adatom which pulls the orbital into a conduction band resonance, resulting in a dipole on the crystal surface. This dipole is oriented with positive charge outward, producing a local depression in the surface barrier which, in turn produces an increase in current. (The externally applied field, which tends to polarize the electron wave function in the opposite direction, is about one order of magnitude lower than the effective field produced by the work function) The local barrier height depression is calculated in zero order as the sum of dipole field and the surface tunnelling barrier. The excess current is then calculated by a three-dimensional WKB method [7], as used in the theory of alpha decay. This includes the well-known centrifugal potential term [8] involving $l(l+1)$ which further lowers the barrier. Here we use, without great justification, the angular momentum value corresponding to the highest filled atomic orbital. Thus there are two effects by which the presence of an adatom increases emission current, the order of magnitude of which is calculable. (We note, also, that the tunnelling distance is slightly shorter for electrons issuing from adatoms than for surface atoms, depending also on the applied field.)

The centrifugal potential is related to the orbital angular momentum and subtracts the term
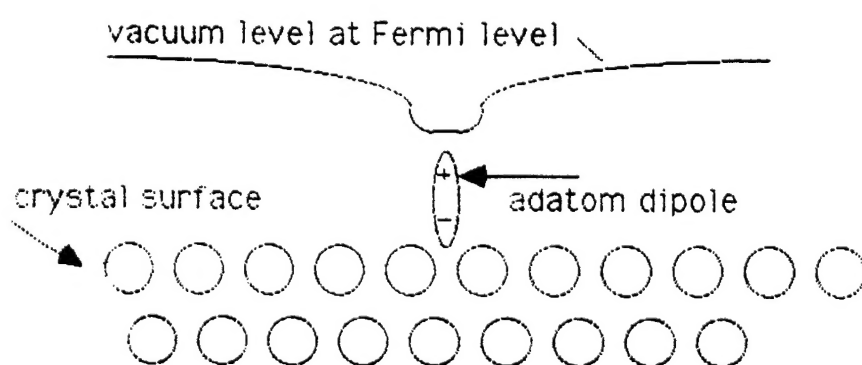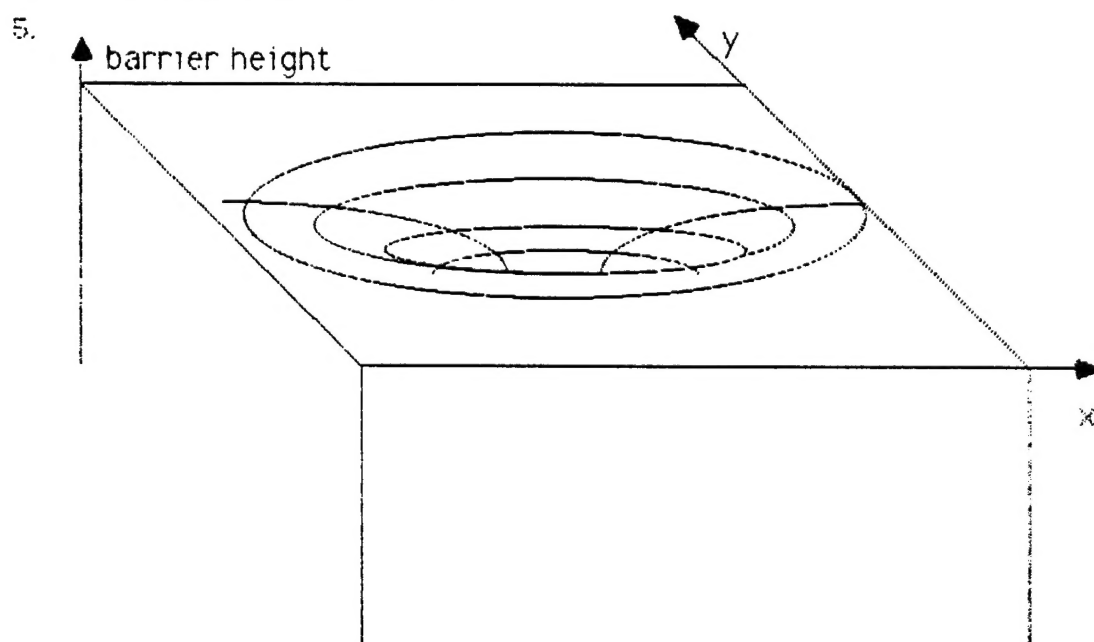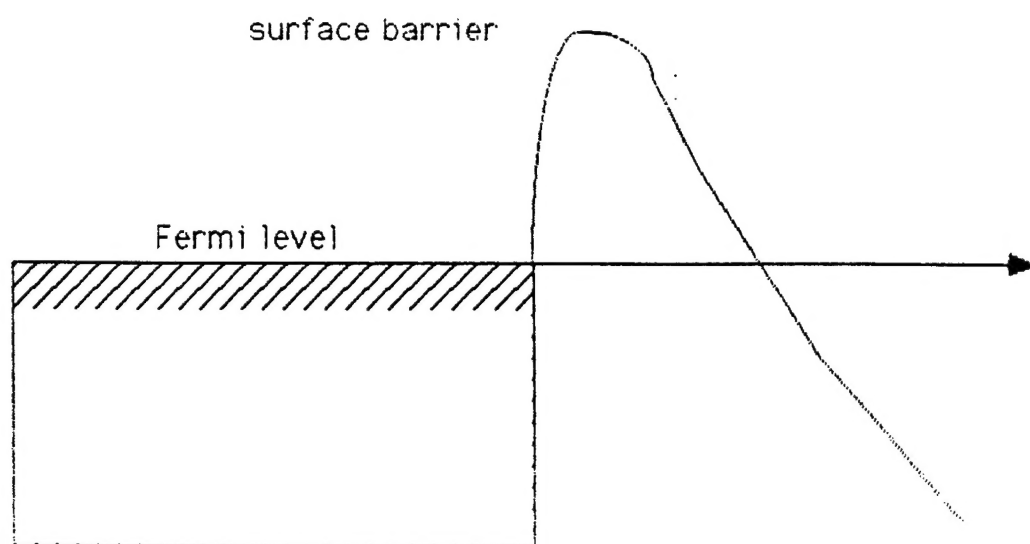
$$V_{centrif} = - \; l(l+1) \, h^2 / 4\pi^2 \, mr^2$$

from the potential V in the WKB expression for the transition rate

$$T = -2 \frac{4\pi^2 m}{h^2} \int_0^{d(E)} dx \sqrt{E - V(x)}$$

(This is Bethe's procedure for calculation of alpha decay of the nucleus [7]

3. CALCULATION OF CURRENT FLUCTUATIONS DUE TO ADATOM ADSORPTION-DESORPTION KINETICS: PREDICTIONS. In ¶ 2 we calculated the extra current emission due to a single adatom on a flat crystal surface. Here we bring into the picture the fact that adatoms are continually adsorbed and desorbed from the surface and that the ordinary surface occupation equilibrium statistics provide values of the mean occupation and of the variance of that occupation[9]. Furthermore, the power spectrum of surface occupation by adatoms is given by the well-known fluctuation-dissipation theorem of irreversible statistical mechanics [10], by means of using the heat of adsorption as the "dissipation" parameter. By combining the power spectrum of surface adatom occupation numbers with the excess tunnelling current due to individual adatoms, as in ¶ 2, we obtain the spectrum of current fluctuations. This is easily seen to be of 1/f form when it is recognized that one can expect the adsorption of an adatom to produce an upward current step, followed by a downward step when desorption occurs. It is noted that the this calculation predicts the current noise well-enough to predict its dependence on experimental quantities such as temperature, pressure, electric field, and emission area.

These considerations are sketched diagrammatically in the following figures:

surface barrier

Fermi level

5.

barrier height

y

x

vacuum level at Fermi level

crystal surface

adatom dipole

4.   CALCULATION OF "SEARCH-LIGHT FLUCTUATIONS": (PREDICTIONS) We apply the
foregoing calculation of flicker noise to a quantitative claculation of "search-light fluctuations"

by considering that the adsorption-desorption kinetics is taking place on a surface composed of crystal facets of different orientations. This means that an emission fluctuation caused by an adatom sends an extra current into a direction which depends on the orientation of that facet. The facet orientations, area, and field then determine the excess current induced by adatoms. We also take into account that the change in facets near the emitter tip changes the field distribution and the facet with high field and low work function predominates

5.   CALCULATION OF EMISSION NOISE ASSOCIATED WITH SURFACE SELF-DIFFUSION:
(PREDICTIONS).   The assumption here is that surface atoms can jump out of lattice positions and move over the surface of crystallographic facets, a process reelated to surface diffusion.   The extra current associated with such an event can be calculated by applying the methods of ¶ 1, and using a random walk treatment of surface diffusion in which Taylor forces are included. This is, of course, a minor extension of the description of the "forming process" given many years ago by Benjamin and Jenkins [11] and Crewe [12].   This is an effect which depends predictably on temperature and field (through the Taylor electrostatics force) and which does not disappear in ultrahigh vacuum when the adsorption rate becomes low.

6.   CONCLUSIONS: We have provided a simple theory of emission noise associated with chemisorption and surface diffusion. It makes definite predictions of power spectrum and amplitude, as a function of ambient partial pressures, temperature, work function, heat of adsorption, etc which can be tested experimentally.

7.   REFERENCES:
[1]   R. Gomer, "Field Emission and Field Ionization" (harvard University Press, Cambridge, Mass, 1961).
[2]   C. Spindt, I. Brodie, L. Hunphrey, and E. R. Westerberg, J. Appl. Phys. 47, 5248, 1985
[3]   W. P. Dyke and W. W. Dolan, Adv. Electronics and Electronic Phys. 8, 180 (1956)
[4]   H. F. Gray, (private communication), 1985
[5]   R. Gomer, Surface Science, 38, 373(1973)
[6]   N. V. Egorov, Sov. Phys. Tech . Phys., 15, 372(1973)
[7]   J. M. Blatt and V. F. Weisskopf, "Theoretical Nuclear Physics", John Wiley (NY 1950), Chapter XII.
[8]   E. Merzbacher, "Quantum Mechanics" John Wiley (NY 1961), p.172
[9]   A. Zangwill, "Physics at Surfaces" Ch. 9 (Cambridge, 1988)
[10]   H. B. Callen and R. F. Greene, Phys. Rev. 86, 702 (1951)
[11]   M. Benjamin and R. O Jenkins, Proc. Roy Soc. London A176, 262(1940)
[12]   A. V. Crewe, D.N. Eggenburger, J. Wall, and L. M. Welter, Rev. Sci. Instr. 39, 576(1968)

8.   PLANS:
a)   A numerical evaluation of the above formulas will be carried out. (next quarter)
b)   A UHV system, now being assembled, will be used to carry out noise experiments on MCNC-grown 1x1 field emitters to compare noise charactristics with the above theory. (This UHV system is funded by UNC-C; experiments will be carried out by Prof. K. Daneshvar, E. E. Department) (following quarter)
c)   The above noise theory will be extended to arrays to calculate the noise figures of field emitter array amplifiers of various designs (following quarter)

4